THE JOURNAL OF PHYSICAL CHEMISTRY C

Article

pubs.acs.org/JPCC

Temperature-Dependent Ordering Phenomena of a Polyiodide System in a Redox-Active Ionic Liquid

Verner K. Thorsmølle,* Jan C. Brauer, Shaik M. Zakeeruddin, Michael Grätzel, and Jacques-E. Moser

Laboratory for Photonics and Interfaces, Institute of Chemical Sciences and Engineering, École Polytechnique Fédérale de Lausanne, CH-1015 Lausanne, Switzerland

ABSTRACT: Iodine added to iodide-based ionic liquids leads to dramatic changes of their physical properties which may have implications for technological applications. Here we study the phase diagram of 1-methyl-3-propylimidazolium iodide, the temperature versus iodine (I_2) concentration. Above a threshold I_2 concentration of 3.9 M, polyiodides are found to be the major determinant of the thermodynamic properties, where nucleation occurs at reduced temperatures leading to a crystalline phase followed by a nematic phase. At the highest concentrations and for increasing temperatures a phonon mode develops which gives indication of mesophases with both improved orientational order of the polyiodide chains and a degree of positional order close to melting. These novel results are important for the fundamental understanding of the physical properties in molten salts and for applications where ionic liquids are used as charge-transporting media such as in batteries and dye-sensitized solar cells.

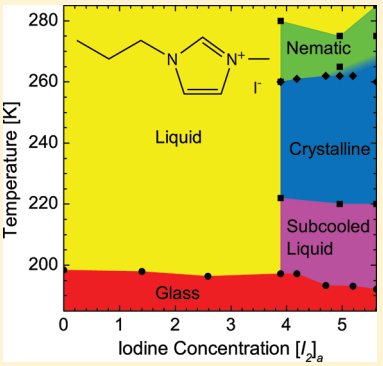

INTRODUCTION

Salts in the liquid phase at room temperature, also known as ionic liquids, possess unique properties that have in recent years earned them considerable attention.[1] The most attractive properties include high ionic conductivity, negligibly low vapor pressure, high thermal and chemical stability, broad electrochemical windows, and nonflammability. These prominent advantages make them versatile alternatives to conventional solvent-based systems. Their potential applications range from fuel cells,[2] electrolytes in solar cells,[3] batteries and supercapacitors,[4] solvents for catalysis and clean chemical synthesis,[5] and solvents for cellulose[6] to heat-transfer fluids and lubricants.[7]

When used as an ion-transporting medium, an anomalously high charge transport efficiency has been observed among the salts which form an ionic liquid containing I^-/I_3^- anions.[8,9] This has been attributed to Grotthuss conduction via the exchange reaction $I^- + I_3^- \rightleftharpoons I_3^- + I^-$ in which I^- and I_3^- ions are displaced without effective mass transfer.[1] In addition, the conductivity rises abruptly by an order of magnitude in the redox active ionic liquid 1-methyl-3-propylimidazolium iodide (PMII) with increasing analytical I_2 concentration $[I_2]_a$ due to increased bond-exchange among the higher polyiodides, I_5^-, I_7^-, and so forth.[1] (The calculated analytical I_2 concentration $[I_2]_a$ takes the volume increase into account when the neutral I_2 is added to the charged PMII melts.[1])

PMII is, as already known, characterized by a liquid subcooling to a glass state upon cooling which is a well-known behavior for imidazolium-based ionic liquids.[10,11] However, when adding I_2 to PMII we discovered that upon heating and for $[I_2]_a$ > 3.9 M—where higher polyiodides are present—PMII passes from the glass to a subcooled liquid phase followed by cold crystallization whereafter it melts to a liquid. In this study we used terahertz time-domain spectroscopy (THz-TDS) in conjunction with differential scanning calorimetry (DSC), which are sensitive to these phases. In particular, we found that the polyiodide chains give rise to a nematic phase during the melting process. At the highest I_2 concentration a phonon mode develops for increasing temperatures whose behavior bares evidence of both improved orientational order as well as a degree of positional order of the polyiodide chains. These ordering phenomena at melting in PMII have similarities to that seen in other physical systems including melting in polymers with long chains and vortex lattice melting in a high-T_c superconductor.[12−14] In addition, a variety of mesophases are observed in ionic liquid crystal and certain salt mixtures.[15,16]

The composition and the physical properties of the PMII melts formed as a function of added I_2 depend on several chemical equilibria as outlined in ref 1. The structure of PMII is shown as an inset to Figure 1. It consists of a PMI^+ cation and an I^- anion. Triiodide (I_3^-) is formed by the addition of I_2 to PMII according to the equilibrium $I^- + I_2 \rightleftharpoons I_3^-$. The species up to $[I_2]_a$ ~3.5 M consists essentially of the ion-paired salt, PMII, of I_2, and of the dissociated ions PMI^+, I^-, and I_3^-. Their concentrations are shown in ref 1, Figure 3a, where PMI^+ and I_3^- increases as a function of added I_2 while PMII and I^- decrease. As the I_2 concentration increases further, the reactions, $I_3^- + I_2 \rightleftharpoons I_5^-$, $I_5^- + I_2 \rightleftharpoons I_7^-$, and so forth, lead to the production of higher polyiodides which have dramatic effects on the physical properties.[1,17] The presence of—predominantly linear—I_5^- becomes detectable for $[I_2]_a$ > 4 M as confirmed by infrared and Raman studies.[1,18,19] In particular, above $[I_2]_a \approx$ 3.9 M, the onset of enhanced Grotthuss

Received: January 4, 2012
Revised: March 5, 2012
Published: March 16, 2012

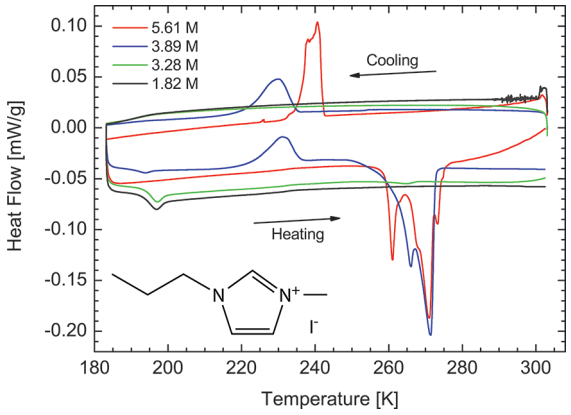

Figure 1. Differential scanning calorimetry data as a function of decreasing (scanning rate: 1 K/min) and increasing (scanning rate: 2 K/min) temperature of PMII/I_2 mixtures at various iodine concentrations $[I_2]_a$. The inset shows the molecular structure of PMII.

conduction among higher polyiodides coincides with the new thermodynamic phases in the T−$[I_2]_a$ phase diagram, that is, the crystalline and nematic phases. This coincidence points to the higher polyiodides being the main responsible component for the thermodynamic and transport properties due to the high iodine/iodide packing density which has been argued to enhance the Grotthuss mechanism by reducing the distance between the iodide/polyiodide species involved in the bond exchange.[1] At $[I_2]_a$ = 3.9 M the polyiodides present a 46 wt % or 25% volume fraction of the mixture implying a densely packed polyiodide medium. Despite the much higher weight content than that typical for rather dilute rigid 3-dimensional networks based on polymer−polymer associations at ∼1%, the thermodynamic behavior of the melts is typical for many polymers and other amorphous compounds.[12,20]

EXPERIMENTAL METHODS

PMII was prepared according to the procedure reported in ref 21. The PMII/I_2 mixtures were prepared by adding the calculated amount of iodine to the PMII, and the solution was then stirred with a magnetic stirring palette for two days to ensure that the iodine would be completely dissolved. Prior to measurements, about 0.2 mL of the PMII/I_2 mixture was introduced into a glass tube, and solvated gases were removed using a slight vacuum of 0.6 Torr at room temperature for about 30 min. The DSC measurements were carried out using a TA Q100 apparatus. The THz-TDS measurements were carried out with an electro-optical terahertz setup for transmission which is described in ref 22. The experiments utilized an amplified Ti:Sapphire laser system operating at 1 kHz, producing nominally 1.0 mJ, 150 fs pulses at 1.5 eV. The sample was contained in a 100-μm-thick cuvette that was mounted inside an optical He cryostat, and the empty cuvette served as a reference. Each complete THz-TDS measurement at one temperature lasted 25 min. The procedure for the analysis of the THz data is described in ref 23.

RESULTS AND DISCUSSION

Figure 1 shows DSC measurements of PMII/I_2 mixtures for various $[I_2]_a$ concentrations. For concentrations less than $[I_2]_a$ ≈ 3.9 M, the PMII melts do not crystallize but enter a glassy state at ∼195 K and reform a liquid upon heating. For $[I_2]_a$ > 3.9 M, the PMII melts are likewise characterized by a glass transition at ∼195 K, but upon heating they pass from the glass to a subcooled liquid phase from which a cold crystallization occurs at ∼225 K followed by melting at ∼265 K. However, for $[I_2]_a$ > 3.9 M and at a sufficiently slow cooling rate (1 K/min), the PMII melts enter a crystalline phase for decreasing temperatures which tends to override the above-mentioned phases until melting at higher temperatures. Importantly, the thermodynamic behavior of the melts is very sensitive to the heating/cooling rate, and crystallization upon cooling will only occur for a sufficiently slow cooling rate <5 K/min. The melting transition is characterized by two melting endotherms indicative of a complex melting behavior which may include remelting of the recrystallized lamellar phase. In the following we investigate the dynamical behavior at and near the melting transition by use of THz-TDS.

Figure 2 shows the real part of the complex conductivity Re($\tilde{\sigma}(\upsilon)$) measured via THz-TDS at various temperatures for

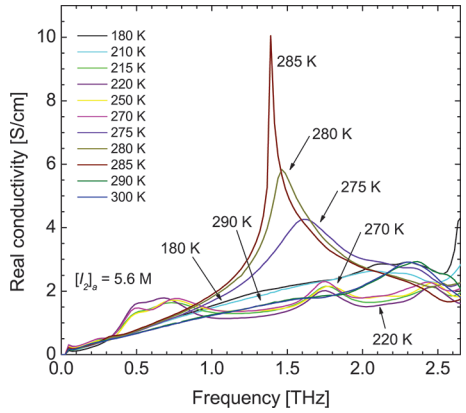

Figure 2. Temperature-dependent terahertz time-domain data: Real part of the complex conductivity as a function of frequency for iodine concentration $[I_2]_a$ = 5.6 M and for increasing temperatures.

$[I_2]_a$ = 5.6 M. The PMII melt was brought into the crystalline state from the subcooled liquid by cooling to 180 K whereafter the temperature was increased in steps as indicated in Figure 2 with the THz-TDS data recorded at each temperature. The 300 K data shows a resonance feature at ∼2.3 THz which is assigned to the linear inner stretch of I_5^-.[1] From 180 to 210 K, the THz spectrum hardly changes, while from 215 to 270 K, the spectrum is dominated by a distinct structure at 500−800 GHz and a resonance feature at ∼1.7 THz indicative of the crystalline phase upon heating. At 275 K, the low-frequency structure vanishes, and the resonance feature is enhanced while shifting to ∼1.6 THz. It becomes increasingly sharper for increasing temperatures with a ∼5-fold amplitude increase, while red-shifting to 1.4 THz, until it at 290 K completely collapses onto the 300 K data. The disappearance of the low-frequency structure suggests the melting of the original crystal structure which coincides with the major endotherm peak in the DSC data, Figure 1, while the subsequent enhancement of the resonance implies reorganization is taking place which improves the order of the polyiodide structure. Importantly, the reordering is clearly initiated at the end of the solid−liquid melting transition as seen from the coinciding last endotherm peak in the DSC measurements (Figure 1). However, it extends ∼10 K into the liquid phase which suggests that even though the system has melted the increased softness allows a reorganization which improves the long-range order while

dx.doi.org/10.1021/jp300105h | J. Phys. Chem. C 2012, 116, 7989−7992

adequate connectivity is still present. Further into the liquid phase all connectivity is lost, and the system transforms from the nematic phase to a pure liquid.

A similar temperature dependence is observed at $[I_2]_a$ = 3.9 M which is shown in Figure 3. The PMII melt is brought to

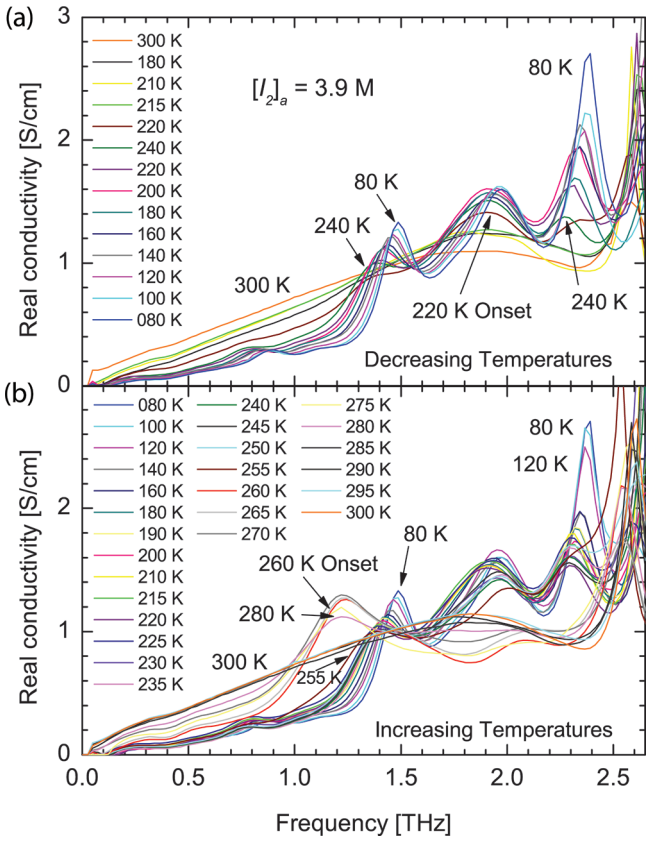

Figure 3. Temperature-dependent terahertz time-domain data: Real part of the complex conductivity as a function of frequency for iodine concentration $[I_2]_a$ = 3.9 M. Upper panel: The temperature is decreased from 300 to 180 K, where after it is increased until 240 K. After the crystal phase has been established by slowly increasing the temperature to 240 K, it is lowered in even steps of 20 K until 80 K. Lower panel: Increasing temperatures.

cold crystallization under the same conditions as for $[I_2]_a$ = 5.6 M, which is seen to commence at 220 K (Figure 3a). After heating to 240 K, the temperature was decreased to 80 K in 20 K steps as indicated. The 300 K data show a broad resonance feature at ∼1.9 THz which is assigned to the absorption of the ion-paired form of PMII and the dissociated forms PMI^+/I^- and PMI^+/I_3^-.[1] In the crystalline state, a structure of three resonances develops in our THz window at ∼1.5 THz, ∼1.9 THz, and ∼2.4 THz which become sharper and more pronounced for decreasing temperatures with a slight blueshift. The increasing temperature data (Figure 3b) resemble that for decreasing temperatures (Figure 3a). Though, at 260 K the three-resonance structure vanishes, while a new resonance appears at ∼1.2 THz. Unlike at $[I_2]_a$ = 5.6 M, it is largely unaffected by temperature until at 285 K it completely collapses onto the 300 K data.

To understand the observed complex melting behavior in polyiodides we briefly discuss that of the better studied polymers. Polymers often exhibit multiple melting behavior, melting–recrystallization–remelting sequences, which depend strongly on the degree of supercooling and the heating rate.[24,25] The morphology of the polymer is determined by the chain structure where under thermodynamic equilibrium the polymer crystals are formed from extended chain crystals. However, most polymer crystals are metastable folded chain crystals which reorganize slowly under temperature changes, and deviation from equilibrium may cause significant reorganization and recrystallization already at crystallization (or annealing and heating). Superheating beyond the equilibrium melting temperature may occur due to their long-chain structure, slow melting, and inherent disorder.[26] Polyiodides can generally be described as constructed from three fundamental building blocks, namely, I^-, I_3^-, and I_2, which casenate easily to form linear chains or more complicated structures.[20] Similar to what has been observed for many polymers, we attribute the multiple endotherm peaks observed in the DSC scans of PMII for $[I_2]_a$ > 3.9 M (Figure 1) to be due to a sequence of melting–recrystallization–remelting of the polyiodide structure. In addition, the enhancement and red-shift of the resonance feature for 5.6 M (Figure 2) which extends ∼10 K into the liquid phase (nematic phase) is attributed to the reorganization of the polyiodide structure to a more ordered state due to superheating. The increasing sharpness of the resonance suggests the development of a phonon-mode, indicative of density correlations in addition to the orientational order of chains. Similar behavior is observed for 3.9 M, except that the resonance feature is broader and largely temperature-independent, indicating less long-range order than for 5.6 M, and does not improve any further during the temperature increase in the nematic phase. This difference in temperature dependence with concentration may be explained by the more densely packed iodide/polyiodide structure at 5.6 M (59 wt % or 37% volume fraction) compared to 3.9 M (46 wt % or 25% volume fraction). Importantly, $[I_2]_a$ = 3.9 M is the threshold concentration for the cold crystallization to occur provided a sufficiently fast cooling rate.

Figure 4 shows the T–I_2 phase diagram of PMII obtained by DSC and THz-TDS measurements. For $[I_2]_a$ < 3.9 M, no crystallization occurs, and the liquid phase extends to 195 K,

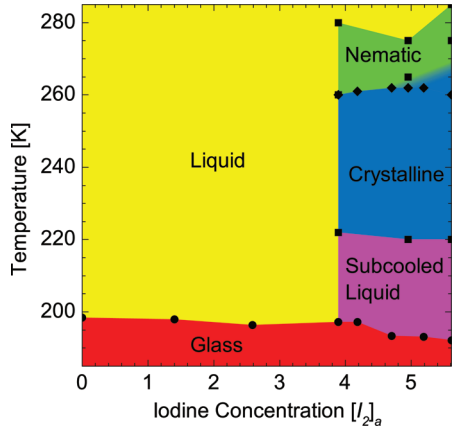

Figure 4. Phase diagram of PMII: Temperature versus iodine concentration $[I_2]_a$. The liquid (light magenta), glassy (red), and crystal (blue) phases are indicated by colors and determined by DSC measurements. The crystal phase above $[I_2]_a$ = 3.9 M is established from a subcooled liquid phase (magenta) for increasing temperatures followed by melting at ∼260 K and a nematic phase (green) probed by THz measurements (heating rate <1 K/min).

dx.doi.org/10.1021/jp300105h | J. Phys. Chem. C 2012, 116, 7989–7992

below which the PMII/I_2 melts enter a glassy state and reform a liquid upon heating. For $[I_2]_a$ > 3.9 M, the glassy state is also obtained, and cold crystallization occurs for increasing temperatures from a subcooled liquid at ∼220 K. At ∼260 K melting sets in which the solution encounters a sequence of melting−recrystallization−remelting transitions. The complex melting is followed by a nematic phase which extends to ∼280 K.

The temperature at which the conductivity abruptly vanishes in the direct current (dc) conductivity hysteresis loop for $[I_2]_a$ = 5.6 M (see ref 17, Figure 3) exactly coincides with crystallization upon cooling (240 K). At 260 K the conductivity is seen to begin gradual recovery, as it enters the nematic phase, until reaching the saturation point at 280 K close to the nematic-liquid interface. Conduction is thus possible in the liquid phase, partly in the nematic phase but not in the crystalline phase.

Reorganization to an improved ordered state just before melting or maintained/enhanced ordering after crossing into the liquid phase are phenomena which have been observed in other classes of physical systems in which disorder plays a central role. For example, in high-T_c superconductors, the softening of the vortex lattice can result in an anomalous enhancement of the critical current density close to the melting transition.[27] Although the exact cause of this "second peak effect" (fishtail effect) is still debated, it is widely regarded as the result of rapid softening of the lattice, the occurrence of plastic deformation, and the presence of disorder.[28] Maintained ordering of *c*-axis correlations of pancake vortices or vortex lines across the melting transition has been observed in low-to-medium anisotropy cuprates as well as enhanced ordering when driving the vortex lattice with a current.[13,29]

CONCLUSIONS

In conclusion, we have investigated the temperature dependence of PMII melts as a function of I_2 concentration using DSC and THz-TDS measurements and have constructed the T−I_2 phase diagram. We found polyidodides to be a major determinant of the thermodynamic properties. For $[I_2]_a$ > 3.9 M, melting of the cold crystalline phase is followed by a nematic phase which at the highest I_2 concentration sees a phonon mode develop as the system softens for increasing temperatures whose behavior is indicative of both improved orientational order of the polyiodide chains as well as a degree of positional order. While improved order has been found in other classes of systems close to melting, this is, to the best of our knowledge, the first observation of a nematic phase and improved ordering phenomena of a polyiodide system at melting.

AUTHOR INFORMATION

Corresponding Author

*E-mail: verner.thorsmolle@epfl.ch.

Notes

The authors declare no competing financial interest.

ACKNOWLEDGMENTS

We thank Christopher Plummer, Paul Dyson, Jason Hancock, N. Peter Armitage, and Björn Lindman for fruitful discussions. We acknowledge financial support by the Swiss National Science Foundation and Marie Curie Reintegration Grant MIRG-CT-2005-014868.

REFERENCES

(1) Thorsmølle, V. K.; Rothenberger, G.; Topgaard, D.; Brauer, J. C.; Kuang, D.-B.; Zakeeruddin, S. M.; Lindman, B.; Grätzel, M.; Moser, J.-E. *ChemPhysChem* **2011**, *12*, 145−149.
(2) Angel, C. A.; Xu, W. *Science* **2003**, *302*, 422−425.
(3) Grätzel, M. *Nature* **2001**, *414*, 338−344.
(4) Seki, S.; Kobayashi, Y.; Miyashiro, H.; Ohno, Y.; Usami, A.; Mita, Y.; Watanabe, M.; Terada, N. *Chem. Commun.* **2006**, 544−545.
(5) Wasserscheid, P.; Welton, T. *Ionic liquids in synthesis*; Wiley-VCH Verlag: Weinheim, 2008.
(6) Lindman, B.; Karlström, G.; Stigsson, L. *J. Mol. Liq.* **2010**, *156*, 76−81.
(7) Ye, C.; Liu, W.; Chen, Y.; Yu, L. *Chem. Commun.* **2001**, 2244−2245.
(8) Kawano, R.; Watanabe, M. *Chem. Commun.* **2005**, 2107−2109.
(9) Bai, Y.; Cao, Y.; Zhang, J.; Wang, M.; Li, R.; Wang, P.; Zakeeruddinm, S. M.; Grätzel, M. *Nat. Mater.* **2008**, *7*, 626−630.
(10) Fredlake, C. P.; Crosthwaite, J. M.; Hert, D. G.; Aki, S. N. V. K.; Brennecke, J. F. *J. Chem. Eng. Data* **2004**, *49*, 954−964.
(11) Fei, Z. F.; Kuang, D. B.; Zhao, D.; Klein, C.; Ang, W. H.; Zakeeruddin, S. M.; Grätzel, M.; Dyson, P. J. *Inorg. Chem.* **2006**, *45*, 10407−10409.
(12) Doi, M.; Edwards, S. F. *The Theory of Polymer Dynamics*; Oxford University Press: New York, 1988.
(13) Thorsmølle, V. K.; Averitt, R. D.; Shibauchi, T.; Hundley, M. F.; Taylor, A. J. *Phys. Rev. Lett.* **2006**, *97*, 237001.
(14) Carlson, E. W.; Castro Netro, A. H.; Campbell, D. K. *Phys. Rev. Lett.* **2003**, *90*, 087001.
(15) Binnemans, K. *Chem. Rev.* **2005**, *105*, 4148−4204.
(16) Henderson, W. A.; Passerini, S. *Chem. Mater.* **2004**, *16*, 2881−2885.
(17) Thorsmølle, V. K.; Topgaard, D.; Brauer, D.-B.; Zakeeruddin, S. M.; Lindman, B.; Grätzel, M.; Moser, J.-E. *Adv. Mater.* **2012**, *24*, 781−784.
(18) Jovanovski, V.; Orel, B.; Jerman, I.; Hočevar, S. B.; Ogoreve, B. *Electrochem. Commun.* **2007**, *9*, 2062−2066.
(19) Jerman, I.; Jovanovski, V.; Šurca Vuk, A.; Hočevar, S. B.; Gaberšček, M.; Jesih, A.; Orel, B. *Electrochim. Acta* **2008**, *53*, 2281−2288.
(20) Svensson, P. H.; Kloo, L. *Chem. Rev.* **2003**, *103*, 1649−1684.
(21) Bonhôte, P.; Dias, A.-P.; Papageorgiou, N.; Kalyanasundaram, K.; Grätzel, M. *Inorg. Chem.* **1996**, *35*, 1168−1178.
(22) Thorsmølle, V. K.; Wenger, B.; Teuscher, J.; Bauer, J. C.; Moser, J.-E. *Chimia* **2007**, *61*, 631−634.
(23) Brauer, J. C.; Thorsmølle, V. K.; Moser, J.-E. *Chimia* **2009**, *63*, 189−192.
(24) Supaphol, P.; Spruiell, J. E. *Polymer* **2001**, *42*, 699−712.
(25) Widmann, G. *Thermochim. Acta* **1987**, *112*, 137−140.
(26) Wunderlich, B. *Thermochim. Acta* **2007**, *461*, 4−13.
(27) Reissner, M.; Lorenz, J. *Phys. Rev. B* **1997**, *56*, 6273−6287.
(28) Mikitik, G. P.; Brandt, E. H. *Phys. Rev. B* **2001**, *64*, 184514.
(29) Thorsmølle, V. K.; Averitt, R. D.; Maley, M. P.; Hundley, M. F.; Koshelev, A. E.; Bulaevskii, L. N.; Taylor, A. J. *Phys. Rev. B* **2002**, *66*, 012519.